CrossMark

Dielectric, Piezoelectric Enhancement and Photoluminescent Behavior in Low Temperature Sintered Pr-Modified $Ba_{0.85}Ca_{0.15}Zr_{0.1}Ti_{0.9}O_3$ Ceramics

RAMOVATAR,[1] INDRANI COONDOO,[2] S. SATAPATHY,[3] NITU KUMAR,[4] and NEERAJ PANWAR [ORCID][1,5]

1.—Department of Physics, Central University of Rajasthan, Bandarsindri, Ajmer, Rajasthan 305817, India. 2.—Department of Physics and CICECO- Aveiro Institute of Materials, University of Aveiro, 3810-193 Aveiro, Portugal. 3.—Laser Materials Section, HBNI, Raja Ramanna Centre for Advanced Technology, Indore 452013, India. 4.—Department of Physics, University of Puerto Rico, San Juan, PR 00931, USA. 5.—e-mail: neerajpanwar@curaj.ac.in

Pristine and 0.04 wt.% Pr_6O_{11} substituted $Ba_{0.85}Ca_{0.15}Zr_{0.1}Ti_{0.9}O_3$ (BCZT) lead-free ceramics have been synthesized by the conventional solid-state reaction method at 1450 and 1300°C sintering temperatures, respectively. The synthesized compounds were characterized by their structural, microstructural, piezoelectric, dielectric and luminescent properties. Coexistence of tetragonal and orthorhombic phases was observed for both pure and Pr doped BCZT compounds. Higher piezoelectric coefficient (d_{33}) ~ 220 pC/N, maximum dielectric constant (ε_m) ~ 4204 and minimum dielectric loss (tanδ) ~ 0.025 were obtained for Pr doped compound as compared to 180 pC/N, 3353 and 0.034 values, respectively, for the undoped BCZT ceramics. Strong photoluminescence emission spectra consisting of blue (489 nm), green (530 nm) and red (602 nm) light emissions were observed in Pr doped compound. Our results demonstrate that Pr_6O_{11} addition in BCZT ceramics is helpful in increasing the electrical properties, inducing the luminescent effect and simultaneously reducing the sintering temperatures of BCZT. The results have been understood in the light of Pr^{3+} ions occupying the Ti^{4+}-sites.

Key words: Lead-free piezoelectrics, dielectric properties, photoluminescence properties

INTRODUCTION

Lead zirconate titanates, Pb(Zr, Ti)O_3 (PZT), a family of piezoelectric ceramics, are the most widely used material in electromechanical conversion technological devices such as sensors, actuators, switches, transducers and filters because of their excellent piezoelectric and dielectric properties close to the morphotropic phase boundary (MPB). An MPB is a coexistence of rhombohedral and tetragonal phases, and it provides the easy directions of polarization rotation.[1] However, lead zirconate titanate ceramics are not environmentally friendly because of the presence of almost 60% quantity of PbO that is carcinogenic in nature. Therefore, it is very much pertinent to develop lead-free piezoelectrics with comparable electrical properties for replacing the lead based ceramics in various applications.[2,3] In the past, lead-free ferroelectric compounds such as $(Bi_{0.5}Na_{0.5})TiO_3$ (BNT), $(K_{0.5}Na_{0.5})NbO_3$ (KNN) and $BaTiO_3$ (BT) based ceramics and their modified specimens have received much attention because of their better piezoelectric (d_{33} = 200–600 pC/N) and dielectric properties.[1,4] Among all the lead-free compounds, Ca and Zr substituted $BaTiO_3$ system $0.5Ba(Zr_{0.2}Ti_{0.8})O_3$-$0.5(Ba_{0.7}Ca_{0.3})TiO_3$ (0.5BZT-0.5BCT) or $Ba_{0.85}Ca_{0.15}Zr_{0.1}Ti_{0.9}O_3$ received considerable

Dielectric, Piezoelectric Enhancement and Photoluminescent Behavior in Low Temperature
Sintered Pr-Modified $Ba_{0.85}Ca_{0.15}Zr_{0.1}Ti_{0.9}O_3$ Ceramics

5871

attention due to much higher piezoelectric coefficient (d_{33} = 620 pC/N) and excellent dielectric properties.[5] Wang et al.[6] reported the best electrical (d_{33} = 650 pC/N, ε_r = 4500 and P_r = 11.69 $\mu C/cm^2$) properties in $Ba_{0.85}Ca_{0.15}Zr_{0.1}Ti_{0.9}O_3$ ceramics. Tian et al.[7] obtained the outstanding piezoelectric (d_{33} = 572 pC/N) and dielectric (ε_r = 4821 and $\tan\delta$ = 0.015) properties in $(Ba_{0.85}Ca_{0.15})(Zr_{0.1}Ti_{0.9})O_3$ ceramic. Keeble et al.[8] carried out the phase diagram investigation of $(Ba_{0.85}Ca_{0.15})(Zr_{0.1}Ti_{0.9})O_3$ ceramic by the high resolution synchrotron x-ray diffraction technique and observed an intermediate orthorhombic phase between a rhombohedral-tetragonal phase. Zhang et al. investigated the phase transitions and piezoelectric behaviour near the MPB region. Two phase transitions were detected by x-ray diffraction, Raman and dielectric permittivity. The observed piezoelectric coefficient was d_{33} = 545 pC/N.[9] Kumar et al.[10] reported a detailed study on the structural phase transformation behavior of this composition under the effect of electric field, stress and temperature. They established the $(Ba_{0.85}Ca_{0.15})(Zr_{0.1}Ti_{0.9})O_3$ system exhibits metastable phases in a wide temperature range, and the large piezoelectric coefficient of the composition is due to the increased fraction of metastable phases increased by the electric field. The main drawback of the $(Ba_{0.85}Ca_{0.15})(Zr_{0.1}Ti_{0.9})O_3$ system is the requirement of much higher sintering temperature between 1400°C and 1600°C which curtails its practical usage. Therefore, it is required to reduce the sintering temperature of BCZT ceramics without compromising the properties. The reduction in the sintering temperature of the pristine BCZT compound has resulted in the significant deterioration of the piezoelectric and electrical properties.[6,11] Other methods adopted to reduce the sintering temperature include the structural modification by the introduction of rare-earth cations. Due to their moderate ionic radii and special electronic structure, rare-earth ions can be easily incorporated at both Ba^{2+}- and Ti^{4+}-sites.[12–14] Moreover, the addition of rare-earth ions in BCZT ceramics has been found to improve the dielectric, piezoelectric and luminescent properties of the host ceramics.[15–19] Among all the rare-earth ions, the Praseodymium (Pr) rare-earth cation has mostly been used as a structural modifier and an activator ion to improve the electrical and luminescent properties of several kinds of perovskite oxides due to its amphoteric nature.[19,20] Besides, this ion has also been used as a sintering aid to reduce the sintering temperatures of the ceramics. Coondoo et al. and Han et al. reported Pr_6O_{11} and Pr_2O_3 tailored $(Ba_{0.85}Ca_{0.15})(Zr_{0.1}Ti_{0.9})O_3$ ceramics sintered at 1350°C and 1400°C with higher piezoelectric coefficients $\sim$ 435 pC/N and $\sim$ 460 pC/N, respectively.[20,21] The main motive behind this work is to investigate the structural, microstructural, piezoelectric, dielectric and luminescent properties of Pr doped BCZT compounds sintered at 1300°C. The

reason for choosing only 0.04 wt.% Pr_6O_{11} as the modifier/substituent in BCZT was that optimal piezoelectric properties were observed for this composition by Coondoo et al.[20]

EXPERIMENTAL DETAILS

The samples were synthesized following the protocol as described in our previous published work [3] except that 0.04 wt.% Pr_6O_{11} modified BCZT pellets were sintered at 1300°C for 2 h duration in this study. The details about the structural (XRD and Raman), surface morphological, ferroelectric and photoluminescent (PL) characterization procedures are also similar to those followed in Ref. [3]. For the present compounds, temperature dependent dielectric permittivity and tangent loss were measured using an Alpha—A high performance modular measurement system (Novocontrol Technologies) at different frequencies in the temperature range 30–230°C. For the piezoelectric measurement, the samples were poled under a 'dc' electric field of 2.5 kV/mm for 20 min in a silicone oil bath at room temperature. The piezoelectric measurement was performed using a PIEZOTEST (d_{33} PiezoMeter System).

RESULTS AND DISCUSSION

Structural and Microstructural Analysis

XRD patterns of the pure and 0.04 wt.% Pr-modified BCZT ceramics are shown in Fig. 1a. Both compounds display the pure perovskite structure without any trace of secondary phase(s), demonstrating Pr diffusion into BCZT crystal lattice. Figure 1b depicts the enlarged view of a peak at $2\theta \sim 45°$ angle. It can be noticed from the figure that both undoped and Pr doped BCZT compounds possess tetragonal and orthorhombic phases at $(200)/(002)_T$ and $(022)/(200)_O$ diffraction peaks, respectively, with varying peak intensity at room temperature. Figure 2a and b exhibits the Rietveld fitted XRD patterns of pristine and Pr doped BCZT compounds. Room temperature structural refinement of both the compounds confirm the tetragonal and orthorhombic phases with $P4mm$ and $Amm2$ space groups in accordance with the results of Fig. 1. Table I displays the structural information such as satisfactory agreement factors (R-factors), goodness of fit (χ^2) and lattice parameters (a, b, c and cell volume) of both compounds. Pr atoms in Pr_6O_{11} may occupy either [Ba^{2+} (1.35 Å)/Ca^{2+} (1.0 Å)]-sites or [Zr^{+4} (0.72 Å)/Ti^{+4} (0.68 Å)]-sites due to their amphoteric behavior. However, in the present case, Pr atoms are more likely to occupy Zr/Ti sites of BCZT ceramic according to the peaks shift towards lower angles resulting in cell volume expansion. The effect of Pr substitution on the crystal structure is seen clearly, however; any effect of lowering the sintering temperature on the crystal structure could not be observed. Further, the
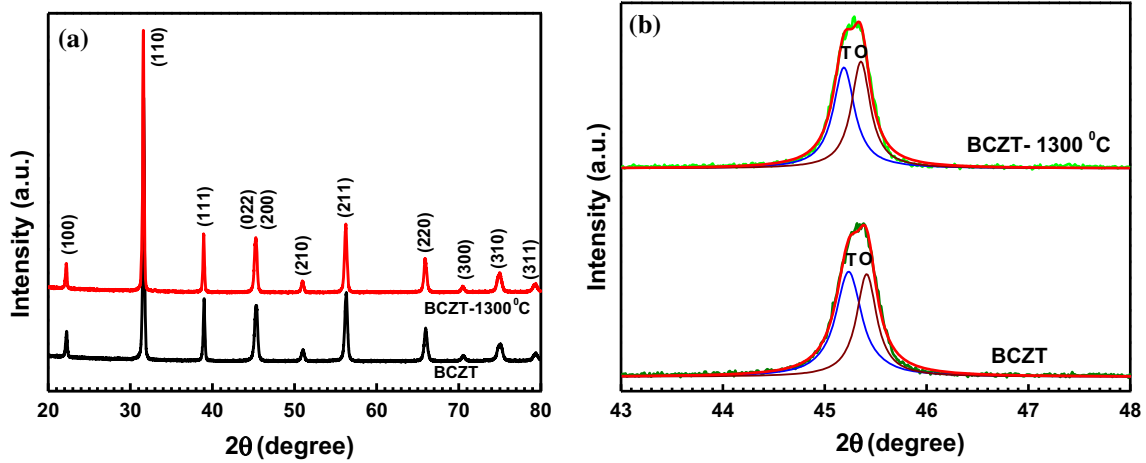
Fig. 1. (a) Room temperature xrd patterns of pure and 0.04 wt.% Pr_6O_{11} modified $Ba_{0.85}Ca_{0.15}Zr_{0.1}Ti_{0.9}O_3$ (BCZT) ceramics. (b) Magnified view of peak at $2\theta \sim 45°$ with Gaussian fitting.

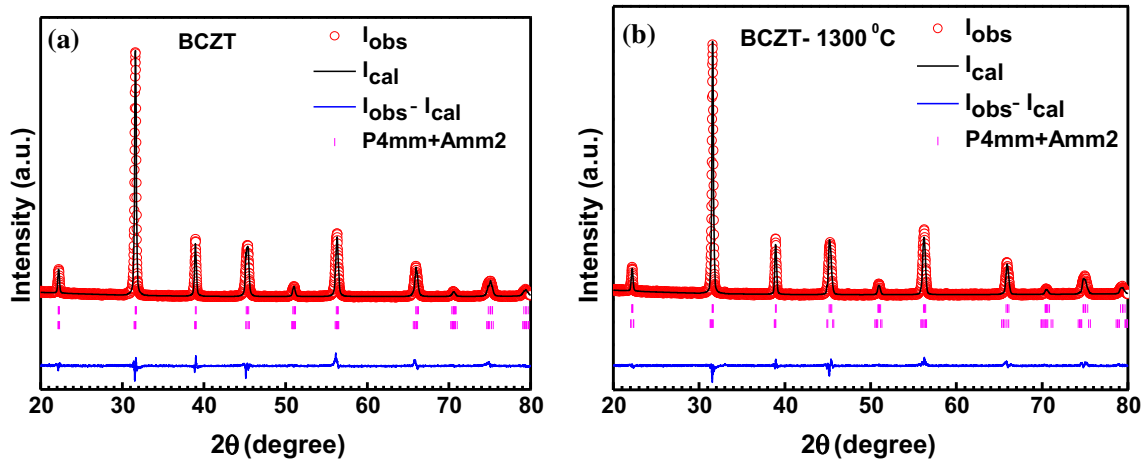Fig. 2. (a) Rietveld fitted profile of $Ba_{0.85}Ca_{0.15}Zr_{0.1}Ti_{0.9}O_3$ (BCZT) and (b) 0.04 wt.% Pr_6O_{11} modified $Ba_{0.85}Ca_{0.15}Zr_{0.1}Ti_{0.9}O_3$ (BCZT) ceramics in tetragonal P4mm and orthorhombic Amm2 structure.

Table I. Parameters obtained from Rietveld refinement of x-ray diffraction data of pure and Pr doped BCZT ceramics at room temperature for co-existing tetragonal (T) and orthorhombic (O) phases with space group P4mm and Amm2

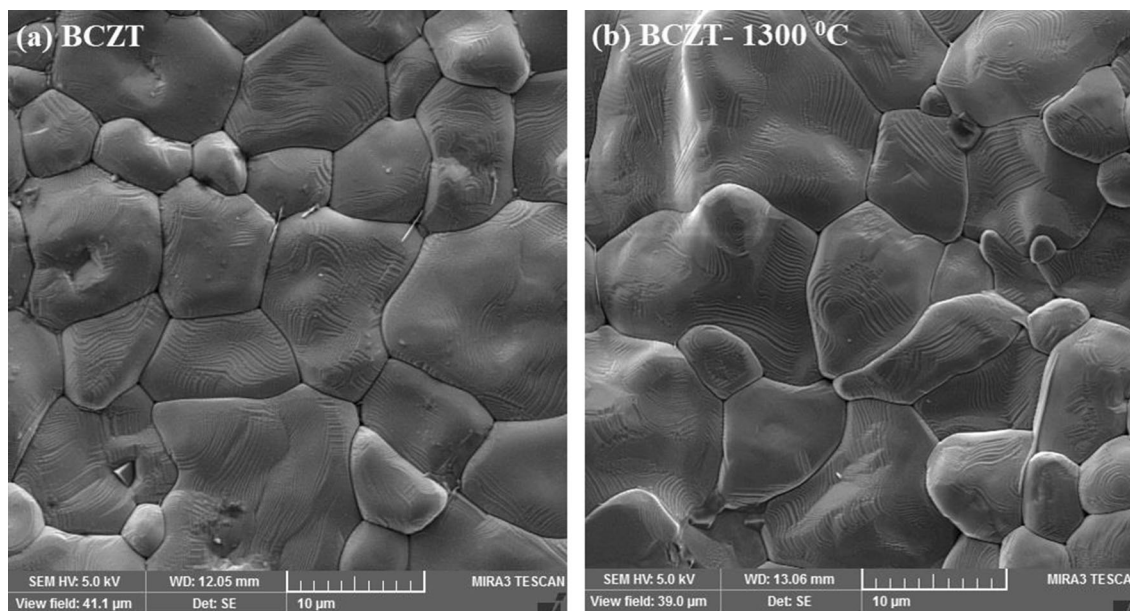|	BCZT		BCZT-1300°C	
Phases	**Mix phase**		**Mix phase**	
Symmetry **Space group**	**T** **P4mm**	**O** **Amm2**	**T** **P4mm**	**O** **Amm2**
a (Å)	3.9987	3.9907	4.0114	3.9770
b (Å)	3.9987	5.6888	4.0114	5.6972
c (Å)	4.0165	5.6678	3.9955	5.7135
V (Å^3)	64.2229	128.662	64.2924	129.458
c/a	1.004	–	0.996	–
R_{exp}	9.54	9.54	9.98	9.98
R_F	5.99	5.99	6.07	6.07
χ^2	2.45	2.45	2.23	2.23

Fig. 3. (a, b) Scanning electron micrographs (SEM) of pure and 0.04 wt.% Pr_6O_{11} modified $Ba_{0.85}Ca_{0.15}Zr_{0.1}Ti_{0.9}O_3$ (BCZT) ceramics.
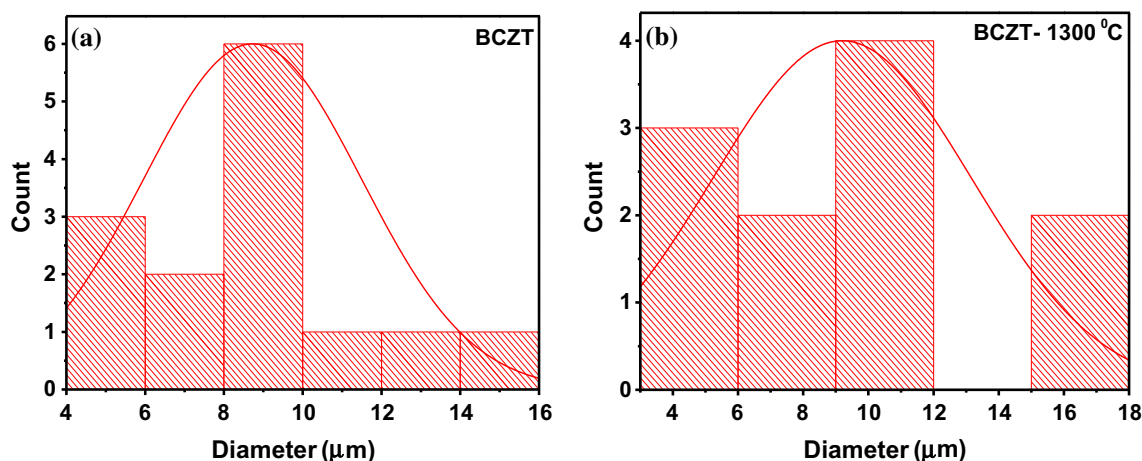

Fig. 4. (a, b) The grain size distribution histograms of pure and 0.04 wt.% Pr_6O_{11} modified $Ba_{0.85}Ca_{0.15}Zr_{0.1}Ti_{0.9}O_3$ (BCZT) ceramics.

density of pure and Pr doped BCZT samples were determined from Rietveld refinement of x-ray diffraction data and experimentally using the Archimedes principle. It was found to increase from 5.51 g/cm^3 for the pristine to 5.65 g/cm^3 for Pr doped compound presumably due to the heavier atomic mass of praseodymium atoms. Figure 3a and b demonstrates the scanning electron micrographs (SEM) of the undoped and Pr doped BCZT samples sintered at 1450°C and 1300°C, respectively. It is clearly observed from the figure that both compounds have well-developed grains with proper grain to grain contact and non-uniform distributions of grains. The average grain size of both samples was determined by using Microsoft Visio 2013 software. Figure 4a and b depict the grain size

distribution histograms of undoped and Pr doped BCZT ceramics. It is evident from the histograms that there is a slight increase in the average grain size with Pr doping. The SEM results are consistent with those reported by Han et al.[21] in Pr_2O_3-doped $(Ba_{0.85}Ca_{0.15})(Zr_{0.1}Ti_{0.9})O_3$ ceramics. This attests that Pr^{3+} ions occupy Ti^{4+}/Zr^{4+}-sites in the BCZT compound in the present study. The reason for no major variation in grain size is as follows: the pristine compound was sintered at 1450°C. At such higher temperature, the enhanced diffusion leads to the grain growth. On the other hand, for the doped compound; the sintering temperature is lower but occupation of Pr^{3+} ions at Ti^{4+}/Zr^{4+}-sites generates oxygen vacancies which are mobile in nature and results in grain growth.

Raman Spectroscopy

Figure 5 illustrates room temperature Raman spectra of pristine and Pr doped BCZT ceramics. The spectra contain A1(TO), B1/E(TO+LO), A1/E(TO), A1/E(LO) Raman active modes in the spectral range 145–290 cm^{-1}, 300 cm^{-1}, 527 cm^{-1} and 730 cm^{-1}, respectively. The interference dip at 171 cm^{-1}, observed due to the coupling between A1 (TO) vibration modes, signifies the presence of a tetragonal phase.[22–24] Besides, the sharp B1/E (TO+LO) mode at 300 cm^{-1} and low intense A1/E (LO) mode at 730 cm^{-1} attest the tetragonality and long-range ferroelectric order of BCZT ceramics. Moreover, the A1/E (LO) phonon mode is also related to bending and stretching of BO_6 octahedra. It has been reported that, in this mode only oxygen ions move in TiO_6 octahedra and change the spacing between Ba^{2+}/Ca^{2+} and Ti^{4+}/Zr^{4+} ions. The behavior of this mode in oxides is describ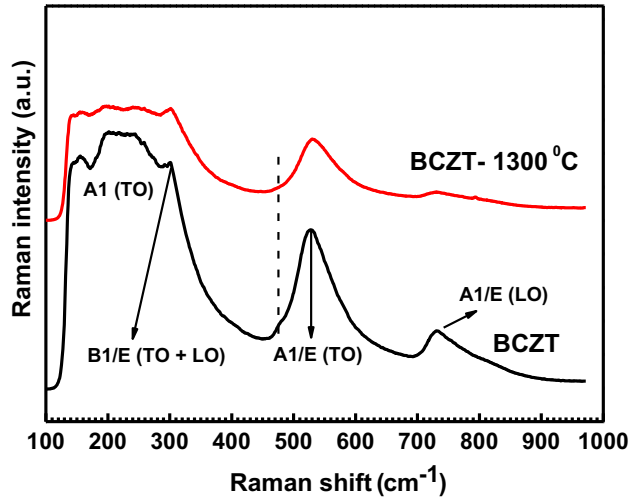ed by short range force constant, long range interactions and masses of the ions involved.[25,26] A1/E (TO) vibration mode at 527 cm^{-1} is assigned to the asymmetric phonon vibration of the Ti-O bond.[24,25] Due to the addition of Pr_6O_{11} in BCZT ceramic, a higher wavenumber shift is noticed for this mode due to the local disorder in the lattice.[20] It can be observed from the figure that intensity and sharpness of this mode decreased in the Pr doped compound. Therefore, a decrease in tetragonality is observed for the Pr doped BCZT compound. This result is consistent with XRD results where a decrease in tetragonality was obtained for a Pr doped BCZT compound. The effect of lowering the sintering temperature along with increased disorder at Ti-sites due to Pr substitution will result in the decrease of the intensity of the Raman spectrum of the doped compound.

Ferroelectric and Piezoelectric Studies of Pr doped BCZT Ceramics

Figure 6a and b display the polarization (P) versus electric field (E) hysteresis loops at room temperature for pure and 0.04 wt.% Pr_6O_{11} modified BCZT ceramics. It is clearly seen from the figure that both samples possess well-saturated hysteresis loops. It is observed that pure BCZT compound exhibits high remnant polarization ($P_r \sim 8.9$ $\mu C/cm^2$). However, a decrease in remnant polarization ($P_r \sim 6$ $\mu C/cm^2$) is observed for the Pr doped compound. The coercive field (E_C) of both the samples are almost the same and equal to 2.5 kV/cm. The decrease in P_r value for the Pr doped sample is mainly attributed to the Pr (3+) substitution at Zr/Ti (4+) sites that acts to break the translational invariance of the polarization and to reduce the coupling of ferroelectrically active TiO_6 octahedra.[27] Pr (3+) substitution, as explained later, will also generate the oxygen vacancies in order to maintain the overall charge neutrality. It will also reduce the polarization. Besides this, lower
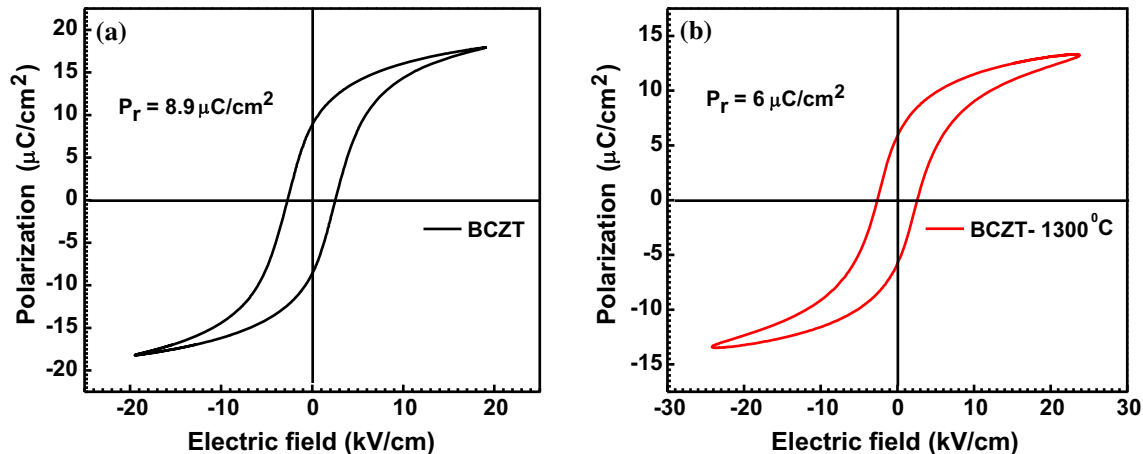

Fig. 5. Room temperature Raman spectra of pure and 0.04 wt.% Pr_6O_{11} doped $Ba_{0.85}Ca_{0.15}Zr_{0.1}Ti_{0.9}O_3$ (BCZT) ceramics over the wave number range 100–1000 cm^{-1}.


Fig. 6. (a, b) Room temperature P-E hysteresis loops of pure and 0.04 wt.% Pr_6O_{11} modified $Ba_{0.85}Ca_{0.15}Zr_{0.1}Ti_{0.9}O_3$ (BCZT) ceramics.

Dielectric, Piezoelectric Enhancement and Photoluminescent Behavior in Low Temperature
Sintered Pr-Modified $Ba_{0.85}Ca_{0.15}Zr_{0.1}Ti_{0.9}O_3$ Ceramics

5875

tetragonality is another reason for the decrease in remnant polarization of Pr doped BCZT compound.[14] Our results are opposite to the behaviour obtained by Coondoo et al.[20] and Han et al.[21] for Pr doped BCZT ceramics. The reason for the difference could be ascribed to the change in the preference of occupancy of Pr^{3+} -ions from Ba^{2+} to Ti^{4+}-sites. It is believed that when Pr is added to BCZT in the form of Pr_6O_{11}, at 1300°C it prefers Ti^{4+}-sites, whereas at higher temperatures it chooses Ba^{2+} sites.

We further measured the piezoelectric constant d_{33} of pristine and Pr doped BCZT poled compounds. The observed values were 180 pC/N and 220 pC/N, respectively. The maximum value of d_{33} for Pr doped BCZT compound may be ascribed to the improved density and grain size of the doped compound.[6]

Dielectric Properties

The temperature and frequency dependent dielectric constant ε_r and tangent loss (tanδ) of pristine and 0.04 wt.% Pr modified $Ba_{0.85}Ca_{0.15}Zr_{0.1}Ti_{0.9}O_3$ (BCZT) samples are shown in Fig. 7a, b, c and d. It can be seen from the Fig. 7a and b that both pure and Pr doped BCZT compounds exhibit two phase transitions viz. orthorhombic to tetragonal (T_{O-T}) and tetragonal to cubic (T_{T-C}) phase. A slight decrease is observed in T_C with Pr doping. Similar results have been reported by Han et al.[21] On the other hand, when Pr^{3+} ion occupies at Ba^{2+} as reported by Coondoo et al.[20] an increase in T_C is observed with Pr doping. The decrease in T_C of this sample is owing to the occupation of Pr^{3+} ion on Ti^{4+}/ Zr^{4+}sites as an acceptor impurity. These acceptor impurities are compensated by oxygen vacancies and expressed as follows[28]:

$$Pr_6O_{11} \overset{TiO_2}{\rightarrow} 6\,Pr'_B + 3V_{\ddot{O}} + xO^{\times}. \qquad (1)$$
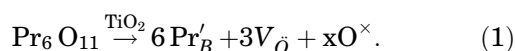
Furthermore, room temperature dielectric constant (ε_r) and peak dielectric constant (ε_m) increase while tangent loss (tanδ) at room temperature decreases for the Pr doped sample. The values of ε_m and tanδ are given in Table II. The increase in maximum dielectric constant value of Pr doped BCZT compound may be ascribed to its higher density and space charge (oxygen vacancies) contribution to the net polarization.[29] These results are contrary to those reported by Coondoo et al. for Pr doped BCZT ceramics sintered at 1350°C and similar to the data of 0.998 $(Ba_{0.99}Ca_{0.01})$ $(Ti_{0.98}Zr_{0.02})O_3$-0.002 $PrO_{1.5}$ obtained by Wang et al.[19] To further investigate the dielectric dispersion and diffuseness of the phase transition of the samples, quantitative analyses were performed. It is well known that for a normal ferroelectric material, dielectric permittivity follows Curie–Weiss law at high temperatures. Curie–Weiss law is given by[20]:

$$\varepsilon = \frac{C}{T - T_C}(T > T_C), \qquad (2)$$

where C is the Curie–Weiss constant and T_C is the Curie temperature. Temperature versus inverse dielectric constant ($1/\varepsilon$) is shown in Fig. 8a and b to analyze the phase transition behavior of the samples. The values of Curie–Weiss constant C obtained from the slope of the temperature versus inverse dielectric constant plots are of the order of 10^5°C which reflects the nature of ferroelectric transition.

To describe the diffuseness of phase transition of these ceramics, a modified Curie–Weiss law was adopted which is given by[30]:

$$\frac{1}{\varepsilon} - \frac{1}{\varepsilon_m} = \frac{(T - T_m)^{\gamma}}{C'}, \qquad (3)$$

where γ is the diffusion coefficient and C' is a Curie–Weiss constant, ε_m is the maximum permittivity and T_m is the permittivity maximum temperature. The value of γ varies from 1 and 2 and gives information about the character of phase transition. The value of $\gamma = 1$ represents normal ferroelectric material while $\gamma = 2$ represents an ideal relaxor ferroelectric material and γ between 1 and 2 represents incomplete diffuse phase transition.[31] The logarithmic form of Eq. 3 would take the following form:

$$\ln\left(\frac{1}{\varepsilon} - \frac{1}{\varepsilon_m}\right) = \gamma \ln(T - T_m) + \ln C'. \qquad (4)$$

Insets of Fig. 8a and b show the linear plots between $\ln(T - T_m)$ and $\ln\left(\frac{1}{\varepsilon} - \frac{1}{\varepsilon_m}\right)$ for both samples. The diffusion coefficient γ is determined from the slope of plots. The parameters obtained by the modified Curie–Weiss law are listed in Table II. An increase in γ value in the Pr doped compound results from the increased disorderness at Ti-sites due to Pr doping. The frequency independent behavior of T_m further attests the absence of the relaxor nature of the studied compounds.

Photoluminescence Spectra

Since the pristine BCZT compound does not contain any photoluminescent (PL) active element, therefore, no spectrum was recorded for this compound.[3] Figure 9a and b displays the room temperature photoluminescence excitation and emission spectra of 0.04 wt.% Pr_6O_{11} modified BCZT sample. The excitation spectrum provides the information about absorption levels of the compounds. The excitation spectrum was recorded between $\sim$ 320–550 nm wavelength range by fixing the detector at 600 nm. The excitation spectrum demonstrates
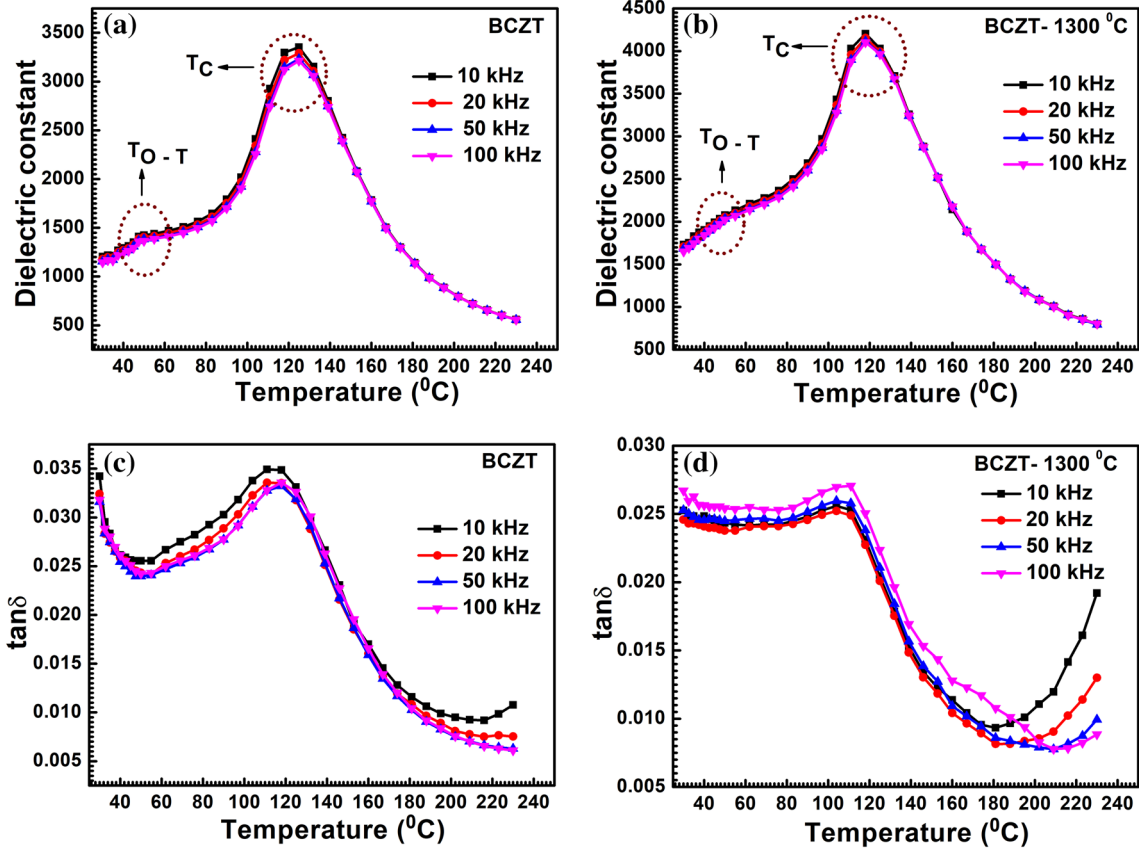
Fig. 7. (a–d) Temperature dependant dielectric constant and dielectric loss of undoped and Pr_6O_{11} modified $Ba_{0.85}Ca_{0.15}Zr_{0.1}Ti_{0.9}O_3$ (BCZT) ceramics at 10 kHz, 20 kHz, 50 kHz and 100 kHz, respectively.

Table II. Parameters obtained from temperature dependent dielectric study of pure and 0.04 wt.% Pr_6O_{11} modified $Ba_{0.85}Ca_{0.15}Zr_{0.1}Ti_{0.9}O_3$ (BCZT) ceramics at 10 kHz

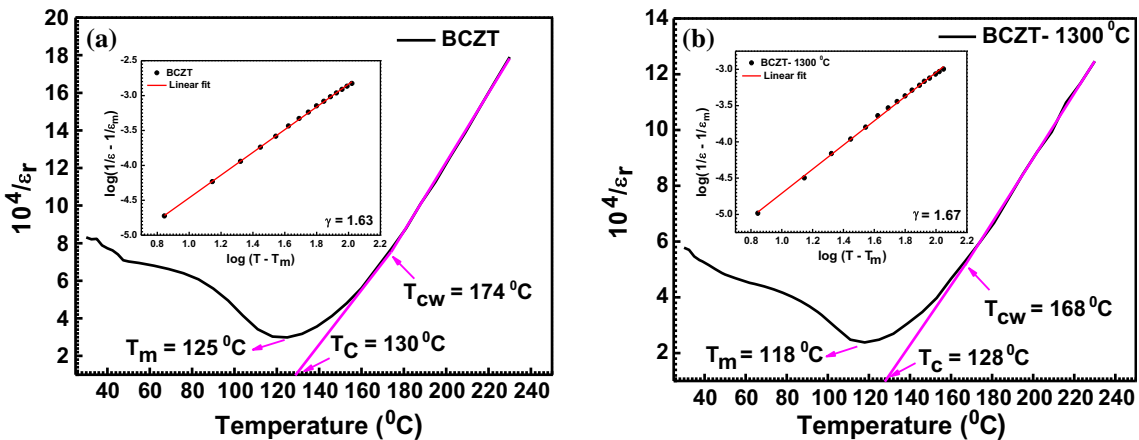| Sample	T_m (°C)	T_0 (°C)	T_{cw} (°C)	ε_m	$\tan\delta$	γ
BCZT	125	130	174	3353	0.034	1.63
BCZT-1300°C	118	128	168	4204	0.025	1.67

Fig. 8. (a, b) Temperature versus inverse dielectric constant for pure and Pr modified $Ba_{0.85}Ca_{0.15}Zr_{0.1}Ti_{0.9}O_3$ (BCZT) ceramics at 10 kHz. Insets are the corresponding plots of $\log(T - T_m)$ against $\log\left(\frac{1}{\varepsilon} - \frac{1}{\varepsilon_m}\right)$.
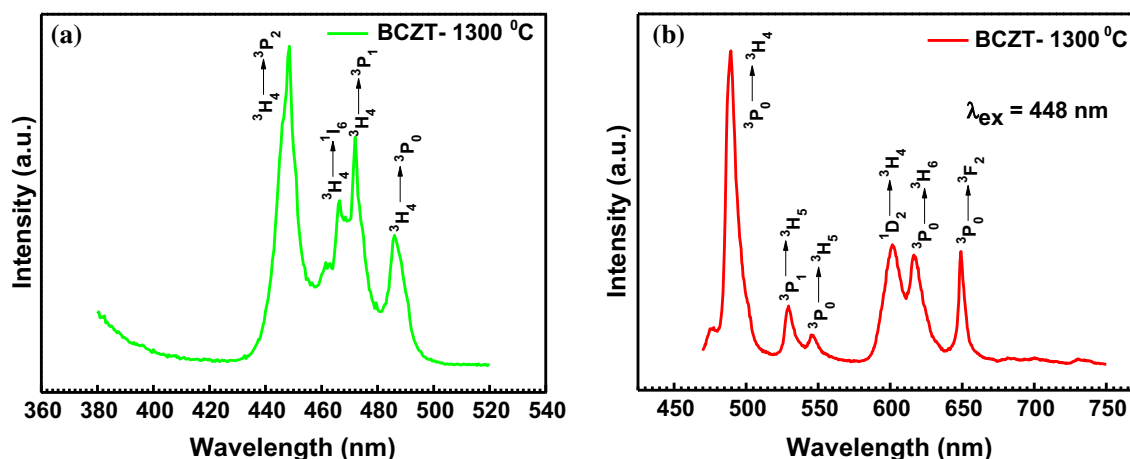
Fig. 9. (a) PL excitation and (b) PL emission spectra of Pr modified Ba$_{0.85}$Ca$_{0.15}$Zr$_{0.1}$Ti$_{0.9}$O$_3$ (BCZT) ceramics.

three sharp peaks at wavenumbers 448 nm, 472 nm and 486 nm, respectively. These peaks are allocated to the transition from the $^3H_4$ absorption to the ^3P_J (J = 0, 1, and 2) excited states of Pr^{3+} ion. Further, a secondary peak located at 466 nm is related to $^3H_4$-$^1I_6$ excitation.[32] The PL excitation peaks in the Pr doped BCZT compound are related to the transitions of 4f electrons of the Pr^{3+} ion. The emission spectrum shown in Fig. 9b was recorded at an excitation of λ_{ex} = 448 nm and consists of strong blue, green and red emission peaks. The blue emission peak is located at 489 nm, the green emission peaks at 530 and 547 nm and the red emission exhibits three peaks centred at 602, 619 and 649 nm, respectively. These blue, green and red emission peaks are ascribed to $^3P_0$-$^3H_4$, $^3P_1$-$^3H_5$, $^3P_0$-$^3H_5$, $^1D_2$-$^3H_4$, $^3P_0$-$^3H_6$, and $^3P_0$-$^3F_2$ transitions, respectively.[32] The reason for the luminescent properties of BCZT ceramic is the addition of Pr rare earth cations. Since, Pr^{3+} is a remarkable activator ion with emission transitions extending from near ultraviolet (UV) to infrared (IR).[33] The calculated CIE (International Commission on Illumination) chromaticity diagram of Pr doped BCZT ceramic excited by 448 nm is shown in Fig. 10. The CIE coordinates (x = 0.41, y = 0.36) induced purplish-red colour emission. Wang et al. have reported the photoluminescent properties of Pr substituted (Ba$_{0.99}$Ca$_{0.01}$)(Ti$_{0.98}$Zr$_{0.02}$)O$_3$ compounds. In one compound Pr substituted Ba^{2+} sites whereas in the other compound Pr goes at Ti- sites. The authors have noticed enhanced luminescent properties in the Ba-site substituted Pr-BCZT compound in comparison to Ti site doped Pr-BCZT system.[19] Similar variation in photoluminescent properties with variation in site occupancy has been reported by us recently.[3] Therefore, we can say that even though our Pr-doped BCZT compound has shown the luminescent behaviour, however, it may be inferior to that for Ba^{2+} site substituted Pr-Ba$_{0.85}$Ca$_{0.15}$Zr$_{0.1}$-Ti$_{0.9}$O$_3$ ceramics studied by Zhang et al.[14]
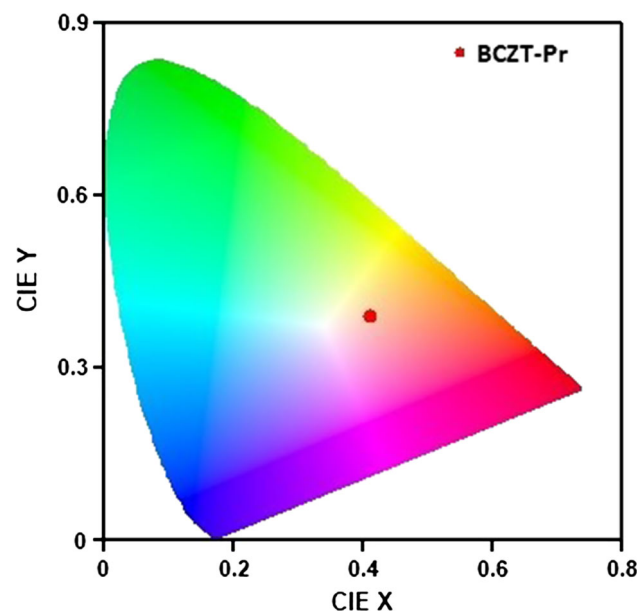

Fig. 10. CIE chromaticity diagram of Pr modified BCZT ceramics.

CONCLUSIONS

Structural, microstructural, dielectric, piezoelectric and luminescence properties of pure and 0.04 wt.% Pr substituted Ba$_{0.85}$Ca$_{0.15}$Zr$_{0.1}$Ti$_{0.9}$O$_3$ ceramics have been investigated at low sintering temperature (1300°C). XRD results at room temperature exhibited the coexistence of tetragonal and orthorhombic phases for pure and Pr modified compounds. XRD results were also corroborated by Raman spectra measured for both compounds. The Pr doped BCZT ceramics exhibited an increase in the piezoelectric coefficient, maximum dielectric constant and decrease in the dielectric loss along with the induction of strong PL emission spectra around 489, 530 and 602 nm under the excitation of a 448 nm laser wavelength. The above properties of

0.04 wt.% Pr modified $Ba_{0.85}Ca_{0.15}Zr_{0.1}Ti_{0.9}O_3$ sintered at relatively lower temperature specifies its usefulness for multifunctional devices.

ACKNOWLEDGEMENTS

REFERENCES

1. I. Coondoo, N. Panwar, H. Amorín, M. Alguero, and A.L. Kholkin, *J. Appl. Phys.* 113, 4107 (2013).
2. K.G. Webber, R. Dittmer, J. Rödel, K.G. Webber, R. Dittmer, W. Jo, and M. Kimura, *J. Eur. Ceram. Soc.* 35, 1659 (2015).
3. Ramovatar, I. Coondoo, S. Satapathy, and N. Panwar, *Ceram. Int.* 44, 1690 (2018).
4. J. Rodel, W. Jo, K.T.P. Seifert, E.M. Anton, T. Granzow, and D. Damjanovic, *J. Am. Ceram. Soc.* 92, 1153 (2009).
5. W. Liu and X. Ren, *Phys. Rev. Lett.* 103, 257602 (2009).
6. P. Wang, Y. Li, and Y. Lu, *J. Eur. Ceram. Soc.* 31, 2005 (2011).
7. Y. Tian, X. Chao, L. Wei, P. Liang, and Z. Yang, *J. Appl. Phys.* 113, 184107 (2013).
8. D.S. Keeble, F. Benabdallah, P.A. Thomas, M. Maglione, and J. Kreisel, *Appl. Phys. Lett.* 102, 092903 (2013).
9. L. Zhang, M. Zhang, L. Wang, C. Zhou, Z. Zhang, Y. Yao, L. Zhang, D. Xue, X. Lou, and X. Ren, *Appl. Phys. Lett.* 105, 162908 (2014).
10. K. Brajesh, M. Abebe, and R. Ranjan, *Phys. Rev. B* 94, 104108 (2016).
11. E. Chandrakala, J. Paul Praveen, B.K. Hazra, and D. Das, *Ceram. Int.* 42, 4964 (2016).
12. C. Chalfouh, S. Zaghal, A. Lahmar, Z. Sassi, N. Abdelmoula, and H. Khemakhem, *J. Alloys Compd.* 686, 153 (2016).
13. T. Kyomen, R. Sakamoto, N. Sakamoto, S. Kunugi, and M. Itoh, *Chem. Mater.* 17, 3200 (2005).
14. Q. Zhang, H. Sun, X. Wang, Y. Zhang, and X. Li, *J. Eur. Ceram. Soc.* 34, 1439 (2014).
15. J. Shi, X. Lu, J. Shao, B. Fang, S. Zhang, Q. Du, J. Ding, X. Zhao, and H. Luo, *Ferroelectrics* 507, 186 (2017).
16. F. Lei, N. Jiang, L. Luo, Y. Guo, Q. Zheng, and D. Lin, *Funct. Mater. Lett.* 08, 1540001 (2015).
17. Z. Wang, W. Li, R. Chu, J. Hao, Z. Xu, and G. Li, *J. Mater. Sci.: Mater. Electron.* 17, 7569 (2017).
18. W. Li, Z. Xu, R. Chu, P. Fu, and G. Zang, *J. Alloys Compd.* 583, 305 (2014).
19. Z. Wang, W. Li, R. Chu, J. Hao, Z. Xu, and G. Li, *J. Alloys Compd.* 689, 30 (2016).
20. I. Coondoo, N. Panwar, H. Amorín, V.E. Ramana, M. Alguerõ, and A. Kholkin, *J. Am. Ceram. Soc.* 98, 3127 (2015).
21. C. Han, J. Wu, C. Pu, S. Qiao, B. Wu, J. Zhu, and D. Xiao, *Ceram. Int.* 38, 6359 (2012).
22. J.P.B. Silva, E.C. Queiros, P.B. Tavares, K.C. Sekhar, K. Kamakshi, J.A. Moreira, A. Almeida, M. Pereira, and M.J.M. Gomes, *J. Electroceram.* 35, 135 (2015).
23. W. Wu, L. Cheng, S. Bai, W. Dou, Q. Xu, Z. Wei, and Y. Qin, *J. Mater. Chem. A* 1, 7332 (2013).
24. W. Zhang, Z. Wang, and X.M. Chen, *J. Appl. Phys.* 110, 064113 (2011).
25. N.K. Karan, R.S. Katiyar, T. Maiti, R. Guo, and A.S. Bhalla, *J. Raman Spectrosc.* 40, 370 (2009).
26. M. Deluca, L. Stoleriu, L.P. Curecheriu, N. Horchidan, A.C. Ianculescu, C. Galassi, and L. Mitoseriu, *J. Appl. Phys.* 111, 084102 (2012).
27. T.Y. Kim and H.M. Jang, *Appl. Phys. Lett.* 77, 3824 (2000).
28. I. Coondoo, N. Panwar, R. Vidyasagar, and A.L. Kholkin, *Phys. Chem. Chem. Phys.* 18, 31184 (2016).
29. V.V. Mitic, V. Paunovic, and V. Pavlovic, *Ferroelectrics* 470, 159 (2014).
30. K. Uchino and S. Nomura, *Ferroelectr. Lett. Sect.* 44, 55 (1982).
31. J.P. Praveen, K. Kumar, A.R. James, T. Karthik, S. Asthana, and D. Das, *Curr. Appl. Phys.* 14, 396 (2014).
32. Y. Wei, Z. Wu, Y. Jia, J. Wu, Y. Shen, and H. Luo, *Appl. Phys. Lett.* 105, 042902 (2014).
33. R. Piramidowicz, I. Pracka, W. Wolinski, and M. Malinowski, *J. Phys.: Condens. Matter* 12, 709 (2000).